ARCHIVES OF BIOCHEMISTRY AND BIOPHYSICS
Vol. 358, No. 2, October 15, pp. 369–376, 1998
Article No. BB980882

Activation of Horse Liver Alcohol Dehydrogenase upon Substitution of Tryptophan 314 at the Dimer Interface

Françoise Strasser,* Joykrishna Dey,† Maurice R. Eftink,† and Bryce V. Plapp*,[1]
Department of Biochemistry, The University of Iowa, Iowa City, Iowa 52242; and †Department of Chemistry, University of Mississippi, University, Mississippi 38677

Received May 28, 1998, and in revised form July 29, 1998

Horse liver alcohol dehydrogenase contains two tryptophan residues per subunit, Trp-15 on the surface of the catalytic domain and Trp-314 buried in the interface between the subunits of the dimer. We studied the contributions of the tryptophans to fluorescence and catalytic dynamics by substituting Trp-314 with a leucine residue and making two compensatory mutations that were required to obtain a stable protein, leading to the triple mutant M303F-L308I-W314L enzyme. The substitutions increased by two- to sixfold the turnover numbers for ethanol oxidation, acetaldehyde reduction, and the dissociation constants of the coenzymes. The rate of the exponential burst phase for the transient oxidation of ethanol increased slightly, but the rate of dissociation of the enzyme–NADH complex still limited turnover of ethanol, as for wild-type enzyme. The three substitutions at the dimer interface apparently activate the enzyme by allowing more rapid conformational changes that accompany coenzyme binding, probably due to movement of the loop containing residues 293 to 298. The emission spectrum of M303F-L308I-W314L enzyme, which contains Trp-15, was redshifted compared to wild-type enzyme. Time-resolved fluorescence measurements with the triple mutant show that the decay of Trp-15 is dominated by a ~7-ns component. In the mutant enzyme with Trp-15 substituted with phenylalanine, the decay of Trp-314 is dominated by a ~4-ns component. Solute quenching data for wild-type enzyme and the mutants show that only Trp-15 is exposed to iodide and acrylamide, whereas Trp-314 is inaccessible. The luminescence properties of the tryptophan residues in the mutated enzymes are consistent with conclusions from studies of the wild-type enzyme [M. R. Eftink, 1992, *Adv. Biophys. Chem.* 2, 81–114].

Key Words: **alcohol dehydrogenase; tryptophan; fluorescence; kinetics; dynamics.**

The structures of the homodimeric horse liver alcohol dehydrogenase EE isoenzyme (ADH)[2] and several ternary complexes are known to high resolution (1–4). Each subunit of the enzyme has two tryptophan residues that are located in different environments and have distinct fluorescence properties. Trp-15 is at the surface of the protein, at the outer edge of the catalytic domain, and Trp-314 is part of the coenzyme binding domain, buried in the subunit interface, which is an apolar core region formed by β-sheet structures from each monomer. The different environments make ADH an interesting protein for luminescence investigations and permit the resolution of the contribution of each emitting center to the fluorescence signal. Results of various luminescence studies with wild-type ADH have been summarized by Eftink (5). In proteins having multiple luminescent groups, however, fluorescence of individual tryptophan residues may interact or overlap and make the attribution of fluorescence properties for each residue uncertain. Therefore, we used site-directed mutagenesis to prepare enzymes with single tryptophan residues and studied the fluorescence and kinetic characteristics of these enzymes.

A mutated enzyme with Trp-15 replaced with Phe (W15F) was prepared earlier (6). Steady-state and time-resolved fluorescence and phosphorescence studies showed that this enzyme had properties, such as quantum yield, emission maximum, and decay times,

[1] To whom correspondence should be addressed. E-mail: bv-plapp@uiowa.edu.

[2] Abbreviations used: ADH, alcohol dehydrogenase; W15F, the substitution of Trp-15 with Phe-15; W314F, the change of Trp-314 to Phe-314; W314L, Trp-314 to Leu-314; M303F-L308I-W314L, triple mutant of Met-303 to Phe-303, Leu-308 to Ile-308, and Trp-314 to Leu-314.

0003-9861/98 $25.00

that were generally in accord with expectations for the contribution of Trp-314 to the fluorescence properties of wild-type enzyme. Now we have substituted Trp-314 in ADH and investigated the luminescence properties of the remaining Trp-15 and the effects of the substitutions on the enzyme kinetics.

Phe is a conservative replacement for Trp, but Leu or Ile often replace Trp, as shown in the sequence alignment of Zn-containing ADHs (7). This alignment also shows that the substitution of Trp-314 is often accompanied with the replacement of Met-303 and Leu-308 by Phe, Leu, or Ile. For example, human ADH6 has Ile-303, Phe-308, and Leu-314; human ADH π has Ile-303, Leu-308, and Ile-314; frog ADH has Phe-303, Ile-308, and Leu-314; and *Escherichia coli* threonine dehydrogenase has Ile-303, Ile-308, and Ile-314. Thus, we prepared the single mutant enzymes (W314F or W314L) and the triple mutant used in these studies.

EXPERIMENTAL PROCEDURES

Materials. Crystalline native horse liver ADH, NAD^+ (grade I, free acid or Li salt), NADH (grade I, disodium salt), and acrylamide (ultrapure grade) were purchased from Boehringer Mannheim; DEAE–Sepharose Fast Flow and SP–Sepharose Fast Flow were from Pharmacia; pyrazole, 2,2,2-trifluoroethanol, and *N*-methylformamide were provided by Aldrich; and potassium iodide was from Fisher Scientific. Restriction enzymes were purchased from New England Biolabs.

Mutagenesis. The expression phagemid of horse liver ADH, pBPE/EqADH (5.2 kb), contains the cDNA (1.5 kb) coding for ADH, under control by a *tac* promoter, and a replication origin for f1 bacteriophage (8). The ADH is expressed in *E. coli* strain XL1-Blue (Stratagene). Mutations were made on recombinant single-stranded DNA template obtained with helper phage VCMS13 (Stratagene) using the Sculptor *in vitro* mutagenesis system (Amersham), which is based on the phosphorothioate method (9, 10), and using T7 DNA polymerase. The oligonucleotides used to introduce the desired mutations were synthesized on a ABI394 DNA synthesizer. A degenerate 30-mer [CTACTGAG*CGGCCG*TACCT(A/T)(G/C)AAAGGAGCT, mutated bases underlined] was designed to transform the TGG codon for Trp-314 into a TTC for Phe, or TTG for Leu, or TAC for Tyr. A new restriction site for *Eag*I (CGGCCG, italicized) was introduced, without changing the amino acid sequence, complementing the *Eag*I site in the multicloning site of the plasmid vector. A 54-mer-[CTCTCT(T/A)TTAATCCTATGTTG(A/T)TTCTGAG*CGGCCG*TACCCTGAAAGGTGCT] was designed to introduce substitutions at positions 303 and 308 of ADH, in addition to the Trp-314 mutation. The TGG codon for Trp-314 was changed to a CTG codon for Leu, the ATG codon for Met-303 and the CTA codon for Leu-308 were changed to degenerate ATT or TTT codons for Ile and Phe, respectively, and a restriction site for *Eag*I was created at position 310 as described for the 30-mer. Four different triple mutants could be obtained. Mutations were detected after digestion of the phagemid by *Eag*I restriction enzyme and confirmed by sequencing of the cDNA using the dideoxy chain termination method with Sequenase Version 2.0 DNA Sequencing Kit (United States Biochemical) and α^{35}S-dATP (Amersham).

Purification of mutant enzymes. Mutant ADHs were purified essentially as previously described for wild-type enzyme (8), except that the enzyme that eluted from the DEAE-Sepharose column was precipitated with 25% polyethylene glycol 4000 and resuspended in 5 mM sodium phosphate buffer, pH 7.5, containing 0.25 mM EDTA, before being loaded onto the SP–Sepharose column. The expression yield for M303F-L308I-W314L triple mutant was about the same as for wild-type enzyme; 36 mg of protein was obtained from 50 g of wet cells harvested from 9 L of culture. During the purification, the mutant and wild-type enzymes behaved similarly. The mutated protein was at least 90% pure as estimated by gel electrophoresis in agarose or polyacrylamide with sodium dodecyl sulfate and migrated at the same position as wild-type enzyme. About 70% of the subunits titrated with NAD^+ in the presence of pyrazole. The mutant enzyme was crystallized by dialysis against 10% ethanol in 10 mM sodium phosphate buffer, pH 7, at 5°C. The tyrosine/tryptophan composition and the protein concentration were determined from spectra of the mutated enzymes in 0.1 M NaOH (11). Tryptophan content was determined by amino acid analysis of samples hydrolyzed with methanesulfonic acid.

Kinetic characterization and data analysis. The concentration of enzyme active sites (N, normality) was determined by titration with NAD^+ in the presence of pyrazole using double difference spectroscopy (12). The concentrations of nucleotides were determined by absorbance at 260 or 340 nm. Ethanol and acetaldehyde were redistilled before use. Initial velocity kinetics were performed at 25°C in 33 mM sodium phosphate buffer, pH 8, containing 0.25 mM EDTA, with a SLM fluorometer (Model 4800C). The change in NADH concentration was monitored with an excitation wavelength of 340 nm and an emission wavelength of 460 nm. The initial velocity data were fitted to a straight line or parabola with the least-squares analysis program provided with the instrument software. The rates were fitted with the appropriate equations with the programs HYPER, SEQUEN, COMP, NONCOMP, UNCOMP (13).

A BioLogic SFM3 stopped-flow instrument was used to measure transient reactions. The rate constant of NADH release from the enzyme–NADH complex (k_{off}) was determined by mixing 17 μN enzyme and 25 μM NADH with NAD^+ (0.15 to 0.5 mM, varied to obtain saturation) and 10 mM pyrazole and by monitoring the formation of enzyme–NAD^+–pyrazole ternary complex at 294 nm. Data were fitted with an equation for a first-order reaction.

Fluorescence studies. Steady-state fluorescence data were recorded on a SLM fluorometer (Model 4800C) at 25°C with 2 mL samples in 33 mM sodium phosphate buffer, pH 8, containing 0.25 mM EDTA. Fluorescence quenching was studied using a 1-nm excitation band at 295 and 8 nm emission at 350 nm for solute quenching and 330 nm for alkaline transition quenching. Solute quenching was studied by adding aliquots of 5 M potassium iodide or acrylamide to a 2-mL protein sample (1–2 μN enzyme). Data were analyzed with the nonlinear least squares regression analysis program NONLIN (C.M. Metzler, The Upjohn Co., Kalamazoo, MI) by fitting the Stern–Volmer equation with or without a term for the inaccessible emitter:

$$F/F_O = f_1/(1 + K_1[Q]) + f_2$$

where F_O and F are the unquenched and quenched fluorescence intensities, [Q] is the molar concentration of the quencher, f_1 and f_2 represent the fractional protein fluorescence for residues 1 and 2, and K_1 is the dynamic quenching constant for residue 1 in the E-Q complex.

The pH dependence of the fluorescence of ADH (1 μN wild-type enzyme or 1.3 μN M303F-L308I-W314L) was monitored between pH 6.8 and 10, in the absence and presence of 100 mM trifluoroethanol and 0.16 mM NAD^+. Buffers were prepared at 0.1 ionic strength and 0.5 mM EDTA; 20 mM $Na_4P_2O_7$ was adjusted to the desired pH with H_3PO_4 and ionic strength with NaH_2PO_4 and Na_2HPO_4 for pH 5.5 to 9, and with 10 mM sodium carbonate buffers above pH 9.

Frequency domain fluorescence lifetime data were collected using an ISS instrument, together with an Innova (Coherent) argon ion laser, which has lines at 300–305 nm. Using an interference filter centered at 290 nm, the effective wavelength of excitation was 300

nm. Emission was collected through a WG335 filter. Intensity decay data were collected at 20°C and analyzed in terms of a bi-exponential decay law, as described elsewhere (14). Likewise, anisotropy decay data were collected with this frequency domain instrument and were analyzed as described elsewhere (15).

RESULTS

Protein properties. The enzymes with the single substitutions, W314F and W314L, were poorly expressed. Moreover, the W314F enzyme was not very stable on storage, and the W314L enzyme had low activity. In contrast, the triple mutant (M303F-L308I-W314L) enzyme that we designed and selected for study was obtained in good yield and was characterized. The extinction coefficient at 280 nm and pH 7 determined for the native triple mutant, as deduced from the spectrum in alkali, was 10,500 N^{-1} cm^{-1} (subunits, 40 kDa), comparable to 10,400 N^{-1} cm^{-1}, calculated from the aromatic amino acid residue composition. (The extinction coefficient for wild-type enzyme is 18,200 N^{-1} cm^{-1} compared to 15,900 N^{-1} cm^{-1} calculated from the composition of the aromatic amino acid residues.) The tyrosine/tryptophan ratio calculated from the spectrum of M303F-L308I-W314L enzyme in 0.1 M NaOH was 3, but amino acid analysis confirmed the presence of four tyrosines and one tryptophan in the mutated enzyme, as compared to four tyrosines and two tryptophans in wild-type. Titration of the active sites of M303F-L308I-W314L ADH yielded a difference extinction coefficient at 293 nm for the enzyme–NAD^+–pyrazole complex of 8200 M^{-1} cm^{-1}, which is comparable to the value of 9000 M^{-1} cm^{-1} for wild-type enzyme (16).

Kinetic characterization. The initial velocity patterns for M303F-L308I-W314L enzyme indicated a sequential bi bi mechanism for ethanol oxidation and acetaldehyde reduction, as described for wild-type enzyme (17, 18). The M303F-L308I-W314L enzyme has 4-fold higher turnover numbers for ethanol oxidation and acetaldehyde reduction compared to wild-type enzyme (Table I). Since Michaelis constants for both substrates are not significantly affected by the mutation, catalytic efficiencies for ethanol oxidation and acetaldehyde reduction are increased by a factor of 5 to 6. The inhibition constants for coenzymes, corresponding to dissociation constants of enzyme–coenzyme complexes, increased in the mutant enzyme (2.5-fold for NAD^+ and 6-fold for NADH), indicating lower affinity for the coenzymes.

Product inhibition data were consistent with competitive inhibition by NAD^+ versus NADH and by NADH versus NAD^+. Dead-end inhibition studies with substrate analogues, 2,2,2-trifluoroethanol and *N*-methylformamide, were used to determine the enzymatic mechanism of the mutated enzyme. Inhibition data with trifluoroethanol were best described as competitive inhibition against ethanol and uncompetitive inhibition against NAD^+. In the reverse reaction, the same patterns applied for *N*-methylformamide, competitive inhibition against acetaldehyde and uncompetitive inhibition against NADH. The ordered bi bi mechanism is consistent with these results (24). The dissociation constants for *N*-methylformamide for M303F-L308I-W314L and wild-type enzymes are similar, whereas the dissociation constant for 2,2,2-trifluoroethanol is five times lower for M303F-L308I-W314L than for wild-type enzyme.

TABLE I

Kinetic Constants for Wild-type and Mutant Alcohol Dehydrogenases[a]

Kinetic constant	Wild-type[b]	M303F-L308I-W314L
K_a (μM)	3.9	27
K_b (mM)	0.35	0.22
K_p (mM)	0.4	0.29
K_q (μM)	5.8	3.5
K_{ia} (μM)	27	68
K_{iq} (μM)	0.5	2.9
V_1 (s^{-1})	3.5	13
V_2 (s^{-1})	47	190
V_1/K_b (mM^{-1} s^{-1})	10	59
V_2/K_p (mM^{-1} s^{-1})	120	660
TN (s^{-1})	2.4	4.0
K_{eq} (pM)	16	38
K_d CF_3CH_2OH (μM)	5.6[c]	1.1
K_d CH_3NHCHO (mM)	1.4[d]	1.3

[a] Initial velocity studies were performed at pH 8.0 and 25°C in 33 mM sodium phosphate containing 0.25 mM EDTA. Coenzyme and substrate concentrations were varied over a ninefold range around the K_m values. Data were fitted to the equation for a sequential bi mechanism with the program SEQUEN (13), and standard errors were ≤20% of the values. K_a, K_b, K_p, and K_q are the Michaelis constants for NAD^+, ethanol, acetaldehyde, and NADH, respectively. V_1 and V_2 are turnover numbers of ethanol oxidation and acetaldehyde reduction, respectively. V_1/K_b and V_2/K_p are catalytic efficiencies for ethanol oxidation and acetaldehyde reduction, respectively. TN is the turnover number in the standard assay (19) based on the active site titration with NAD^+ in the presence of 10 mM pyrazole. K_i values are product inhibition constants determined with varied coenzyme concentrations in a fourfold range at a fixed concentration of the other substrate. Data were fitted with the equation for competitive inhibition (COMP, ref. 13). The equilibrium constant was calculated from $K_{eq} = (V_1K_pK_{iq}[H^+])/(V_2K_bK_{ia})$ and should have a value of 9 pM (17); the differences between the calculated and known values indicate that the cumulative errors in the kinetic constants are small. K_d values are dissociation constants for trifluoroethanol and *N*-methylformamide obtained in dead-end inhibition studies. K_d CF_3CH_2OH was calculated from $K_{ii}/(1 + K_b/[\text{ethanol}])$ from uncompetitive inhibition against NAD^+ or $K_{is}/(1 + K_{ia}/[NAD^+])$ from competitive inhibition against ethanol. K_d CH_3NHCHO was calculated from $K_{ii}/(1 + K_p/[\text{acetaldehyde}])$ from uncompetitive inhibition against NADH or $K_{is}/(1 + K_{iq}/[\text{NADH}])$ from competitive inhibition against acetaldehyde.

[b] Kinetic constants reported by Dworschack and Plapp (20).

[c] From Shore *et al.* (21); Cook and Cleland (22).

[d] Fan and Plapp (23).

TABLE II

Kinetic Constants for Transient Oxidation of Ethanol[a]

	Wild-type[b]	M303F-L308I-W314L
Rate constant (s^{-1})	180	230 ± 20
K_m (mM)	4.1	31 ± 6

[a] Burst reactions were measured with 15 μN enzyme mixed with 2 mM NAD^+ and varied concentrations of ethanol (6.7 to 50 mM) and monitoring the formation of NADH (ϵ = 5.5 mM^{-1} cm^{-1} at 328 nm), which is the isoabsorptive point for free and enzyme-bound forms of NADH (25). Data were analyzed with the equation for a first-order reaction followed by a zero-order steady state and fitted to the Michaelis–Menten equation in order to obtain the maximal rate at saturation.

[b] Sekhar and Plapp (26).

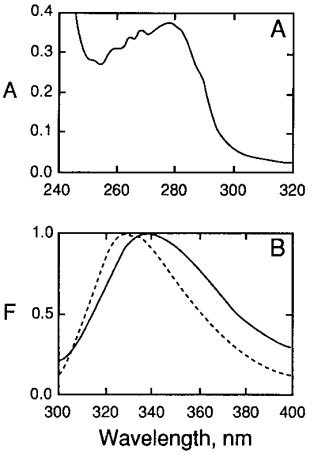

FIG. 1. Spectra for wild-type and M303F-L308I-W314L enzymes. (A) UV-absorbance spectrum for 32 μN triple mutant. (B) Normalized fluorescence emission spectra for 1.2 μN wild-type enzyme (- - -) and 9.3 μN M303F-L308I-W314L enzyme (—) with an excitation wavelength of 295 nm and 1 nm resolution.

Transient kinetics were used to determine the rate constant for dissociation (k_{off}) of NADH from the enzyme–NADH complex. This rate constant was measured by trapping the free enzyme released from the enzyme–NADH complex with saturating NAD^+ and pyrazole, where the rate of formation of the enzyme–NAD^+–pyrazole complex corresponds to the rate of dissociation of NADH. The rate constant for NADH dissociation was 14 s^{-1}, a value very close to the turnover number of ethanol oxidation (V_1 = 13 s^{-1}, Table I). These results suggest that NADH release from the enzyme–NADH complex is the rate-limiting step for the overall reaction, as described for wild-type enzyme (17, 18).

We also used stopped-flow kinetics to investigate the transient burst for ethanol oxidation by M303F-L308I-W314L enzyme, measuring the appearance of the enzyme–NADH complex and NADH at 328 nm (Table II). Ethanol was oxidized with an initial burst with an apparent first-order rate constant of 230 s^{-1}, followed by a steady-state increase in absorbance controlled by the rate of dissociation of NADH from the enzyme–NADH complex. Wild-type enzyme has a transient rate constant of 180 s^{-1} (26).

Luminescence characteristics of tryptophan residues. The M303F-L308I-W314L enzyme was studied in order to compare the fluorescence of Trp-15 with the characteristics dissected from studies of the wild-type protein (see Ref. 5 for a review of fluorescence properties of wild-type ADH). The emission spectra of M303F-L308I-W314L and wild-type ADH are shown in Fig. 1. The mutant enzyme has an emission maximum of 340 nm, due to Trp-15, whereas the wild-type enzyme has a maximum at 330 nm. The emission spectrum of the W15F enzyme also has a maximum at 330 nm, due to Trp-314 (6). These spectra provide direct evidence that Trp-15 has a much redder emission than Trp-314, as concluded previously from selective solute and energy transfer quenching and wavelength-dependent time-resolved fluorescence measurements (27–33). In a similar manner, fluorescence excitation spectra (not shown) of the mutant and wild-type enzymes show the excitation of Trp-15 to be blueshifted with respect to that of Trp-314, a result that is consistent with previous indirect dissection studies (6).

Solute quenching of the mutant enzyme was studied to determine whether the emission of Trp-15 has the expected accessibility to acrylamide and iodide (27, 29, 30). The relative fluorescence intensities were determined as a function of iodide and acrylamide concentration, as shown in Fig. 2. The data are best described by fits to the Stern–Volmer equation with the parameters listed in Table III. Iodide could quench 100% of

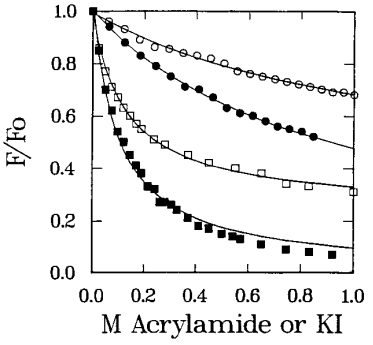

FIG. 2. Solute quenching of the steady-state fluorescence of wild-type and M303F-L308I-W314L enzymes. Excitation was at 295 nm and emission at 350 nm. Potassium iodide quenching of 1.2 μN wild-type (○) and 1.9 μN M303F-L308I-W314L (●) enzymes. Acrylamide quenching of 0.9 μN wild-type (□) and 2.3 μN M303F-L308I-W314L enzymes (■). Data for wild-type enzyme were analyzed with the Stern–Volmer equation with a term for the second, inaccessible component.

the fluorescence of M303F-L308I-W314L enzyme (as extrapolated to saturating and experimentally inaccessible concentrations of quencher), whereas only 69% of the fluorescence of wild-type ADH could be quenched. Likewise, acrylamide could quench 100% of the M303F-L308I-W314L enzyme fluorescence compared to 75% of the fluorescence of the wild-type enzyme. The dynamic quenching constants, K, for a particular quenching agent were similar for the two enzymes with Trp-15 and were substantially smaller for the enzyme with Trp-314 (Table III). The data clearly indicate that the quenching is associated with the solute-accessible Trp-15, whereas the inaccessible component in wild-type or W15F enzymes is associated with Trp-314.

The pH dependence of the steady-state fluorescence can also characterize the contributions of Trp-15 and Trp-314. Previous studies showed a pH-dependent quenching reaction, with 45% of the fluorescence quenched above a pK_a of 9.6 (34, 35). This alkaline quenching has been attributed to energy transfer quenching of Trp-314 upon deprotonation of a tyrosine residue (34, 35). In contrast to the alkaline quenching seen for wild-type ADH, no quenching is seen for the M303F-L308I-W314L mutant between pH 6.7 and 10. The fluorescence of wild-type enzyme is also quenched by about 50% upon formation of a ternary complex with NAD^+ and 2,2,2-trifluoroethanol (35). Since there is a redshift in the fluorescence of wild-type ADH upon forming this ternary complex, it is believed that the quenching by coenzyme binding is due primarily to quenching of Trp-314, which is located closer to the coenzyme binding site than is Trp-15. Only 17% of the fluorescence of the M303F-L308I-W314L mutant (data not shown) was quenched upon forming the ternary complex with NAD^+ and trifluoroethanol, a result that is consistent with the above explanation for quenching by coenzyme binding to wild-type enzyme. Furthermore, there is 30–35% quenching of fluorescence of the wild-type enzyme upon forming the ternary complex with NAD^+ and pyrazole, compared with 15–20% quenching of the triple mutant on forming the same ternary complex, and there is 70% quenching of wild-type protein fluorescence upon forming a ternary complex with NADH and isobutyramide, compared to only 30% quenching of the fluorescence of the triple mutant. Each of these results indicates that the binding of either coenzyme causes a significantly greater degree of quenching of the internal Trp-314 than of the surface Trp-15, a result that can easily be explained if the quenching occurs by resonance energy transfer, since Trp-15 is located approximately 25 Å from the nicotinamide or adenine rings of the bound coenzymes, whereas Trp-314 is approximately 15 Å away. (Both distances are within the same subunit, which are the shortest distances).

Frequency domain fluorescence measurements were made on the mutant and wild-type enzymes to characterize the fluorescence lifetime of each tryptophan residue and to determine if the decay profile of the wild-type can be explained as a simple sum of contributions from each residue. Shown in Fig. 3 are phase and modulation data for the two enzymes. In both cases the data were

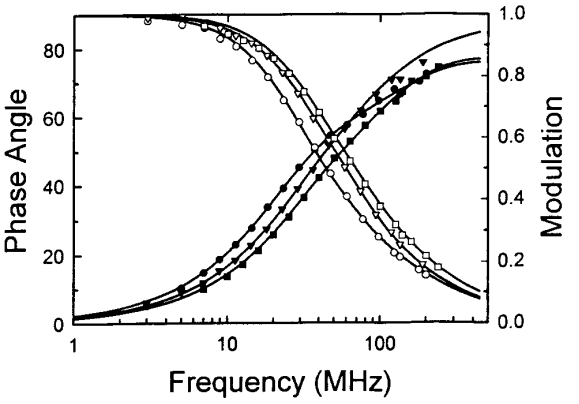

FIG. 3. Frequency domain fluorescence lifetime data for M303F-L308I-W314F enzyme (●, ○), wild-type enzyme (▽, ▼), and W15F enzyme (■, □). The closed symbols are phase angle data; the open symbols are modulation data. The solid lines are biexponential decay fits with parameters given in Table III.

TABLE III

Fluorescence Parameters for Wild-type and Mutant Forms of ADH

	Wild-type	M303F-L308I-W314L	W15F[a]
Emission Max (nm)	330	340	328
Lifetime data			
τ_1 (ns)	7.22 ± 0.27	6.75 ± 0.12	4.30 ± 0.12
τ_2 (ns)	3.75 ± 0.05	1.33 ± 0.06	1.14 ± 0.06
f_1	0.348 ± 0.002	0.885 ± 0.002	0.852 ± 0.004
Anisotropy data[b]			
ϕ_1 (ns)	49 ± 5	53 ± 6	40
$r_{0,1}$	0.296 ± 0.003	0.272 ± 0.003	0.271
ϕ_2 (ns)	0.5 ± 0.2	0.7 ± 0.2	0.7
$r_{0,2}$	0.024 ± 0.006	0.041 ± 0.006	0.038
Iodide quenching			
K_1 (M^{-1})	0.82 ± 0.10	1.1 ± 0.01	0.28
f_1	0.69 ± 0.05	1.00 ± 0.01	⟨1⟩[c]
Acrylamide quenching			
K_1 (M^{-1})	7.5 ± 0.4	9.9 ± 0.4	1.25
f_1	0.75 ± 0.01	1.03 ± 0.02	⟨1.0⟩

[a] Data taken from Eftink *et al.* (6).

[b] The data were fit to a bi-exponential anistropy decay equation (15) where the amplitudes are $r_{0,1}$ and $r_{0,2}$ and the corresponding slow and fast rotational correlation times are ϕ_1 and ϕ_2.

[c] The value was fixed at 1.0 for the fitting.

fitted to a bi-exponential decay law. For wild-type ADH, the two lifetimes were $\tau_1 = 7.22$ ns and $\tau_2 = 3.75$ ns, with f_1, the fractional contribution associated with τ_1, equal to 0.348. These values are in good agreement with several previous determinations by both pulse-decay and frequency-domain lifetime measurements (30–33, 36). For M303F-L308I-W314L, the data were fitted with $\tau_1 = 6.75$ ns, $\tau_2 = 1.33$ ns, and $f_1 = 0.885$. That is, the long τ_1 of 7 ns is dominant in the mutant and is nearly the same as the long τ_1 for wild-type ADH. This confirms previous assignments of wild-type ADH decay profile in terms of a long τ for Trp-15 and a shorter τ for Trp-314. Also shown in Fig. 3 are previously published data for the W15F mutant of ADH, which contains Trp-314 but not Trp-15 (6). The W15F enzyme shows a blue emission with maximum of 328 nm, reduced accessibility to acrylamide quenching, and a dominant τ of 4.3 ns, which is reasonably similar to τ_2 found for wild-type ADH (and attributed to Trp-314).

Differential polarized phase and modulation data (anisotropy decay data) were determined for M303F-L308I-W314L and wild-type enzymes (data not shown). For both enzymes the data were fitted to a bi-exponential (nonassociated) anisotropy decay law. In both cases the anisotropy decays were dominated by a long rotational correlation time, with ϕ_1 of about 50 ns, which is attributed to global rotation of the entire protein molecule. Both proteins show a small amplitude of rapid motion with a ϕ_2 of approximately 0.5–0.7 ns. This short ϕ_2 can be attributed to rapid, segmental motion of the tryptophan residue. In both enzymes the amplitude associated with this ϕ_2 is small, but this amplitude appears to be somewhat larger for Trp-15 in the M303F-L308I-W314L enzyme than in wild-type enyzme.

DISCUSSION

Kinetics. The kinetic data suggest that the ordered bi bi mechanism described for wild-type enzyme is maintained in the M303F-L308I-W314L enzyme. However, the turnover numbers and dissociation constants for coenzymes are increased 2- to 6-fold in the triple mutant, indicating changes in catalytic dynamics. It is significant that the rate constant for NADH dissociation is increased to 14 s^{-1}, which accounts for the increased turnover number for the forward reaction (V_1 = 13 s^{-1}). The rate constant is about 3.5-fold higher than for wild-type enzyme and is reflected also in the increased dissociation constant for the enzyme–NADH complex (K_{iq}, Table I). The dissociation of the enzyme–NADH complex is rate-limiting in the overall reaction, just as for wild-type enzyme. This conclusion was supported by the observation of a transient burst for ethanol oxidation by M303F-L308I-W314L enzyme, which was similar to that for wild-type enzyme (26). The increased activity probably reflects increased rates of conformational changes that occur during coenzyme binding and release. Limited kinetic studies with the W15F enzyme revealed no major differences between the two enzymes (6).

Effects of tryptophan substitutions in ADH. Two compensatory mutations were required to obtain a stable enzyme when Trp-314 was substituted with Leu. The M303F-L308I-W314L enzyme, in which Phe-303, Ile-308, and Leu-314 correspond to the residues found in frog ADH (37) was stable and active. Modeling based on the three-dimensional structure of the horse enzyme suggests that substitutions at positions 303 and 308 might compensate for the structural change resulting from the replacement of Trp-314 by the smaller Leu residue (Fig. 4A). Note that the indole ring of Trp-314 makes contacts (<4.2 Å) with Leu-279, Ile-291, Met-303, and Leu-301 of the same subunit and with Trp-314 and Leu-308 of the other subunit (2). Although the M303F-L308I-W314L enzyme was similar to wild-type enzyme, the triple mutant appears to have more flexibility than the native enzyme, as indicated by the faster rate of dissociation of NADH. This may result from altered movement of the loop involving residues 293 to 298, which flips during formation of ternary complexes due to rotations in phi–psi angles (39). Colonna-Cesari *et al.* (40) have noted that this loop must move in order to accommodate the closing of the active site cleft when the catalytic domain rotates toward the coenzyme binding domain. Figure 4B compares the apo- and holo-enzyme structures and shows that Val-294 and Pro-295 have almost exchanged positions. This conformational change results in very different interactions with the dimer interface, and it is reasonable that the substitutions in the triple mutant should affect the rate of change or the initial and final structures. Residues 292, 294, 306, 309, and 318 participate in binding coenzyme and substrate, and the positions of these residues should affect catalytic events.

Fluorescence properties. The fluorescence of Trp-15 in the triple mutant has the features expected from the structure of the protein and the spectral assignments for the two tryptophan residues in the wild-type protein. Eftink (5) has summarized the various wavelength dependence, solute quenching, and time-resolved fluorescence studies that have led to a characterization of Trp-15 as having a red emission (maximum at about 340 nm), a large exposure to solute quenchers, and a long fluorescence lifetime of about 7 ns whereas Trp-314 has a blue emission (maximum of 330 nm), a very low exposure to solute quenchers, and a fluorescence lifetime of 3–4 ns. These characteristics are consistent with Trp-15 being located on the protein surface and Trp-314 being buried at the subunit interface.

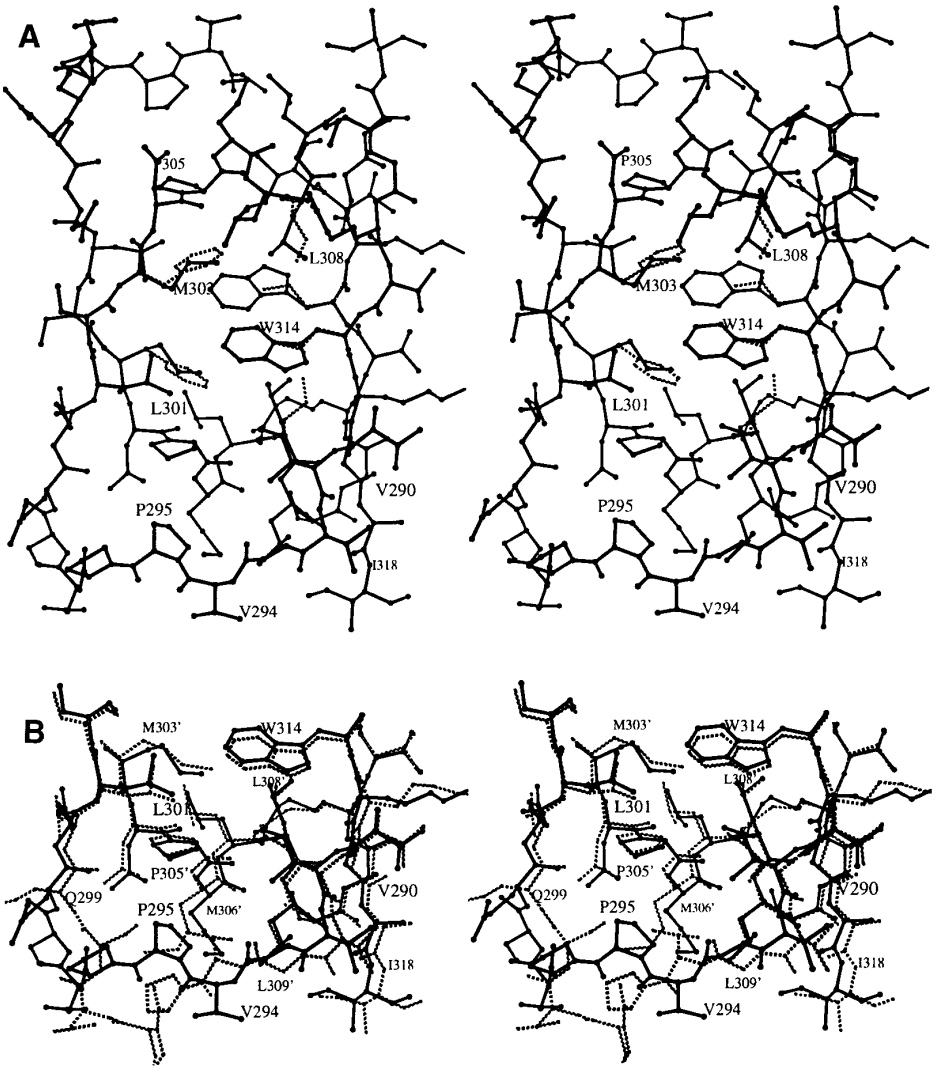

FIG. 4. Dimer interface of alcohol dehydrogenase. (A) Comparison of the interface between subunits in the wild-type holo-enzyme (—) and a model of the triple mutant (- - -). The view is perpendicular to interface, which is in the plane of the paper, and the molecular two-fold axis is horizontal between residues 303 and 314. (B) Comparison of one end of the dimer interface in the apo-enzyme (- - -) and holo-enzyme (—). The residues with primed numbers are from the second subunit. The coordinates for the holo-enzyme are for the enzyme–NADH-3–butylthiolane 1-oxide complex solved at 1.66 Å (entry 3BTO in the Brookhaven Protein Data Bank; Ref. 4) and the coordinates for apo-enzyme are based on data to 2.4 Å (entry 8ADH in the Brookhaven Protein Data Bank). The coenyzme binding domain (residues 176–290 and 300–314) of the apo-enzyme was superimposed onto the holo-enzyme using the program O (38). Other views of the loop have been presented (39, 40). The figure was prepared with BOBSCRIPT, a modified version of MOLSCRIPT (41).

The studies presented here for the triple mutant, which has only Trp-15, are consistent with this assignment. The mutant has a red emission, which is 100% accessible to iodide and acrylamide quenchers, and a dominant fluorescence lifetime of about 7 ns. Also, the fluorescence anisotropy decay of Trp-15 in the triple mutant shows a larger amplitude associated with rapid, segmental motion than does the wild-type protein. This is consistent with Trp-15 having a small amount of rotational freedom, which is more than that experienced by Trp-314.

We presented previously some fluorescence studies with the W15F mutant of ADH, which retains Trp-314 (6). Fluorescence properties of this mutant are included in Table III. As expected, the fluorescence of W15F is relatively blue and has an average fluorescence lifetime of 4 ns. Solute quenching studies showed Trp-314 in this mutant to be relatively buried, but not to the extent expected from studies with wild-type ADH. The combined results with these two mutant forms of ADH generally support the previous dissections of the fluorescence properties of Trp-15 and Trp-

314 in the wild-type protein. The mutations apparently did not significantly affect the dynamic properties of the remaining tryptophans.

ACKNOWLEDGMENTS

This work was supported by NSF Grants MCB 95-06831 (B.V.P.) and MCB 94-07167 (M.R.E.). We thank the University of Iowa Protein Structure Facility for the amino acid analyses and the use of the SLM4800 spectrofluorometer.

REFERENCES

1. Eklund, H., Nordström, B., Zeppezauer, E., Söderlund, G., Ohlsson, I., Boiwe, T., Söderberg, B.-O., Tapia, O., Brändén, C.-I., and Åkeson, Å. (1976) *J. Mol. Biol.* **102,** 27–59.
2. Ramaswamy, S., Eklund, H., and Plapp, B. V. (1994) *Biochemistry* **33,** 5230–5237.
3. Al-Karadaghi, S., Cedergren-Zeppezauer, E., Hövmuller, S., Petratos, K., Terry, H., and Wilson, K .S. (1994) *Acta Crystallogr.* **D50,** 793–807.
4. Cho, H., Ramaswamy, S., and Plapp, B. V. (1997) *Biochemistry* **36,** 382–389.
5. Eftink, M. R. (1992) *Adv. Biophys. Chem.* **2,** 81–114.
6. Eftink, M. R., Wong, C.-Y., Park, D.-H., Shearer, G. L., and Plapp, B. V. (1994) *Proc. SPIE* **2137,** 120–126.
7. Sun, H. W., and Plapp, B. V. (1992) *J. Mol. Evol.* **34,** 522–535.
8. Park, D.-H., and Plapp, B. V. (1991) *J. Biol. Chem.* **266,** 13296–13302.
9. Nakamaye, K., and Eckstein, F. (1986) *Nucleic Acids Res.* **14,** 9679–9698.
10. Taylor, J. W., Ott, J., and Eckstein, F. (1985) *Nucleic Acids Res.* **13,** 8764–8785.
11. Beaven, G. H., and Holiday, E. R. (1952) *Adv. Protein Chem.* **7,** 319–386.
12. Theorell, H., and Yonetani, T. (1963) *Biochem. Z.* **338,** 537–553.
13. Cleland, W. W. (1979) *Methods Enzymol.* **63,** 103–138.
14. Eftink, M. R., and Ghiron, C. A. (1987) *Biophys. J.* **52,** 467–473.
15. Eftink, M. R., Gryczynski, I., Wiczk, W., Laczko, G., and Lakowicz, J. R. (1991) *Biochemistry* **30,** 8945–8953.
16. Shearer, G. L., Kim, K., Lee, K. M., Wang, C. K., and Plapp, B. V. (1993) *Biochemistry* **32,** 11186–11194.
17. Dalziel, K. (1963) *J. Biol. Chem.* **238,** 2850–2858.
18. Wratten, C. C., and Cleland, W. W. (1963) *Biochemistry* **4,** 2442–2451.
19. Plapp, B. V. (1970) *J. Biol. Chem.* **245,** 1727–1735.
20. Dworschack, R. T., and Plapp, B. V. (1977) *Biochemistry* **16,** 111–116.
21. Shore, J. D., Gutfreund, H., Brooks, R. L., Santiago, D., and Santiago, P. (1974) *Biochemistry* **13,** 4185–4190.
22. Cook, P. F., and Cleland, W. W. (1981) *Biochemistry* **20,** 1797–1805.
23. Fan, F., and Plapp, B. V. (1995) *Biochemistry* **34,** 4709–4713.
24. Cleland, W. W. (1963) *Biochem. Biophys. Acta* **67,** 104–137.
25. Theorell, H., and Bonnichsen, R. (1951) *Acta Chem. Scand.* **5,** 1105–1126.
26. Sekhar, V. C., and Plapp, B. V. (1990) *Biochemistry* **29,** 4289–4295.
27. Abdallah, M. A., Biellmann, J.-F., Wiget, P., Joppich-Kuhn, R., and Luisi, P. L. (1978) *Eur. J. Biochem.* **89,** 397–405.
28. Laws, W. R., and Shore, J. D. (1978) *J. Biol. Chem.* **253,** 8593–8597.
29. Eftink, M. R., and Selvidge, L. A. (1982) *Biochemistry* **21,** 117–125.
30. Ross, J. B. A., Schmidt, C. J., and Brand, L. (1981) *Biochemistry* **20,** 4369–4377.
31. Knutson, J. R., Walbridge, D. G., and Brand, L. (1982) *Biochemistry* **21,** 4671–4679.
32. Demmer, D. R., James, D. R., Steer, R. P., and Verrall, R. E. (1987) *Photochem. Photobiol.* **45,** 39–48.
33. Eftink, M. R., Wasylewski, Z., and Ghiron, C. A. (1987) *Biochemistry* **26,** 8338–8346.
34. Laws, W. R., and Shore, J. D. (1979) *J. Biol. Chem.* **254,** 2582–2584.
35. Eftink, M. R. (1986) *Biochemistry* **25,** 6620–6624.
36. Eftink, M. R., and Hagaman, K. A. (1986) *Biochemistry* **25,** 6631–6637.
37. Cederlund, E., Peralba, J. M., Parés, X., and Jörnvall, H. (1991) *Biochemistry* **30,** 2811–2816.
38. Jones, T. A., Zou, J.-Y., Cowan, S. W., and Kjeldgaard, M. (1991) *Acta Crystallogr.* **A47,** 110–119.
39. Eklund, H., Samama, J.-P., Wallén, L., Brändén, C.-I., Åkeson, Å., and Jones, T. A. (1981) *J. Mol. Biol.* **146,** 561–587.
40. Colonna-Cesari, F., Perahia, D., Karplus, M., Eklund, H., Brändén, C.-I., and Tapia, O. (1986) *J. Biol. Chem.* **261,** 15273–15280.
41. Kraulis, P. (1991) *J. Appl. Crystallogr.* **24,** 946–950.